



HAL
open science

s-Tetrazine derivative exhibiting unprecedented polymorphism-dependent emission properties

Yuna Kim, Clémence Allain, Régis Guillot,, Pierre Audebert

► **To cite this version:**

Yuna Kim, Clémence Allain, Régis Guillot,, Pierre Audebert. s-Tetrazine derivative exhibiting unprecedented polymorphism-dependent emission properties. *Journal of Photochemistry and Photobiology A: Chemistry*, 2023, 439, pp.114629. 10.1016/j.jphotochem.2023.114629 . hal-04087314

HAL Id: hal-04087314

<https://hal.science/hal-04087314>

Submitted on 3 May 2023

HAL is a multi-disciplinary open access archive for the deposit and dissemination of scientific research documents, whether they are published or not. The documents may come from teaching and research institutions in France or abroad, or from public or private research centers.

L'archive ouverte pluridisciplinaire **HAL**, est destinée au dépôt et à la diffusion de documents scientifiques de niveau recherche, publiés ou non, émanant des établissements d'enseignement et de recherche français ou étrangers, des laboratoires publics ou privés.

s-Tetrazine derivative exhibiting unprecedented polymorphism-dependent emission properties

Yuna Kim ^{a*}, Clémence Allain ^{b*}, Régis Guillot ^c, Pierre Audebert ^b

a Faculty of Engineering, Utsunomiya University, 7-1-2 Yoto, Utsunomiya, Tochigi 321-8585, Japan

b Université Paris-Saclay, ENS Paris-Saclay, CNRS, PPSM, 91190 Gif-sur-Yvette, France

c Université Paris-Saclay, CNRS, Institut de chimie moléculaire et des matériaux d'Orsay, 91405 Orsay, France

* Corresponding authors.

E-mail addresses: kimyuna@cc.utsunomiya-u.ac.jp (Y. Kim), clemence.allain@ens-paris-saclay.fr (C. Allain).

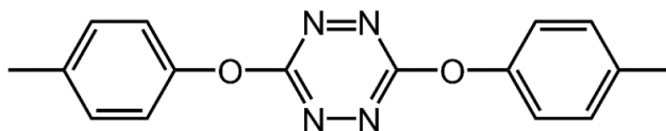
Keywords: S-tetrazine ; Polymorphism ; Thermoresponsive photoluminescence ; Flexible crystal

ABSTRACT

The first example of a tetrazine derivative exhibiting emission color-tunable crystals upon external stimuli such as heat and an organic solvent is described. Bis(4-methylphenoxy)tetrazine (**1**) forms several crystalline phases by heating and cooling processes accompanying unprecedented photoluminescence color transitions including green, yellow, red, and traditional orange colors. These thermoresponsive polymorphisms and colors could be also reversibly recovered to their original state by solvent vapor annealing. The formation of mild excimer-like species and energy state transitions (much-stabilized ground state than the S1 state) presumably contributed to the unique bathochromic and hypsochromic shifts, respectively. In addition, a novel mechanical feature from **1**-the formation of flexible crystals- was achieved, which plausibly originated from the unique *T*-shape arrangement of the tetrazine rings and the phenyl rings observed in the molecular packing.

1. Introduction

s-Tetrazine derivatives are small fluorophores based on electrondeficient heterocycles. Their electroactive and fluorescent properties have been attracting huge attention for the applications of chemosensors [1,2] and electrochemical fluorescence switching (electrofluorochromic) devices [3–5]. Recently, luminescent tunability in condensed phases that can change their photophysical properties in response to external stimuli because of transitions of molecular arrangement has been considered a highly intriguing topic [6–8]. Unconventional photophysical functions as well as facile applications are expected in condensed phases that have been hardly achieved in solution states. However, little attention has been paid to tetrazines in condensed states such as crystalline and/or liquid-crystalline states and their external-stimuli responsive photophysical properties. In particular, crystalline phase-dependent emission transitions in tetrazine-based luminophores triggered by thermal or mechanical stimuli have never been reported to the best of our knowledge. Herein we report the first example of a tetrazine derivative, the bis(4-methylphenoxy)tetrazine (**1**) shown in Scheme 1, exhibiting emission color-tunable crystals upon external stimuli such as heat and organic solvent. In addition to the traditional orange luminescence of stetrazines, multi colors including yellowish-green, yellow, and reddishorange were obtained by heating and cooling the **1** crystal and reversing the luminescence by solvent vapor annealing process. In addition, an unprecedented mechanical feature from **1**- the formation of bendable crystals- was attained, which plausibly originated from the unique *T* shape arrangement of the tetrazine rings and the phenyl rings observed in the molecular packing.



Scheme 1. Formula of tetrazine **1**.

2. Experimental

s-Tetrazine derivative **1** was synthesized according to the previously reported route [9,10]. All organic solvents for solution state photophysical characterizations were of spectroscopic grade (purchased from Sigma-Aldrich) and used as received without further purification. Poly(methyl methacrylate) (PMMA, M.W.ave 120 K) and polystyrene (PS, M.W.ave 280 K) were obtained from Sigma-Aldrich. **1** (0.1 wt%) was blended into the chloroform solution of each polymer (10 wt%) and drop-cast onto glass slides. Transparent polymer films based on monodispersed **1** were fully dried under vacuum at r.t. overnight. Heat treatment and luminescence observation of crystalline power of **1** were carried out with a hot stage (Mettler Toledo F82HT) and a hand-held UV lamp (AS ONE, model Handy UV Lamp SLUV- 4) with a wavelength of 365 nm, respectively. The DSC (differential scanning calorimetry) was measured using a Hitachi DSC 7020 under a nitrogen atmosphere. Powder X-ray diffraction measurement was conducted with a Rigaku SmartLab. UV–visible absorption spectra were recorded on an Agilent CARY 5000 spectrophotometer. Steady-state fluorescence spectra were measured using Fluorolog-3 (Horiba Jobin-Yvon). Time-resolved fluorescence measurements were conducted with a Hamamatsu Photonics Quantaaurus-Tau. Quantum yields in solution were calculated using Rhodamine 6G in ethanol as the reference ($\Phi_F = 0.95$). A digital optical microscope to observe bendable crystals was a Keyence VHX5000. Red crystals of **1** were obtained after crystallization from a CH_2Cl_2 / hexane mixture. X-ray diffraction data for compound **1** was collected by using a VENTURE PHOTON100 CMOS Bruker diffractometer with Micro-focus $\text{Cu K}\alpha$ radiation ($\lambda = 1.54178 \text{ \AA}$). High-quality needle crystal was mounted on a glass fiber in a random orientation. The data were corrected for Lorentz polarization and absorption effects. The structures were solved by direct methods using SHELXS-97 [11] and refined against F^2 by full-matrix least-squares techniques using SHELXL-2018 [12] with anisotropic displacement parameters for all non-hydrogen atoms. Hydrogen atoms were located on a difference Fourier map and introduced into the calculations as a riding model with isotropic thermal parameters. All calculations were performed by using the Crystal Structure crystallographic software package WINGX [13]. The title compound crystallizes in the monoclinic space group $P 2_1/n$ with half a molecule per asymmetric unit, due to an inversion center (located at the tetrazine ring center). The crystal data collection and refinement parameters are given in Table S1, and an ORTEP drawing of compound **1** is shown in Figure S1. CCDC 2219490 contains the supplementary crystallographic data for this paper. These data can be obtained free of charge from the Cambridge Crystallographic Data Centre and Fachinformationszentrum Karlsruhe via <https://www.ccdc.cam.ac.uk/structures/>.

3. Results and discussion

The luminescence color transition behavior of **1** crystalline powder upon thermal stimulus is featured in Fig. 1. Initially, the crystallization of **1** from dichloromethane afforded a reddish-orange emitting crystalline form (referred to RO-form), as always observed with dialkoxytetrazines [14]. The RO-form lost its photoluminescence (nonemissive form) upon heating to an isotropization temperature of around 120 °C. Upon subsequent cooling, surprising photoluminescence was witnessed affording unprecedented yellowish-green color (G-form) at the first appeared crystalline phase at around 100

°C. Further gradual cooling led to the yellow photoluminescence color (Y-form) which appeared going from 70 °C to r.t. Relaxation of the sample at r.t. over 6 h resulted in the emission color changed to still another form, emitting yellowish-orange color (YO-form). We could drive the system back to the photoluminescence color quite close to the original RO-form exhibiting deep orange color (O-form) by organic solvent vapor annealing such as chloroform at room temperature. Fig. 1 shows the images illustrating the fluorescence color variations under a 365 nm UV lamp upon thermal treatment and solvent vapor annealing. In addition, the most blue-shifted greenish emission color could be isolated by supercooling to 5 °C from the melt state at 120 °C.

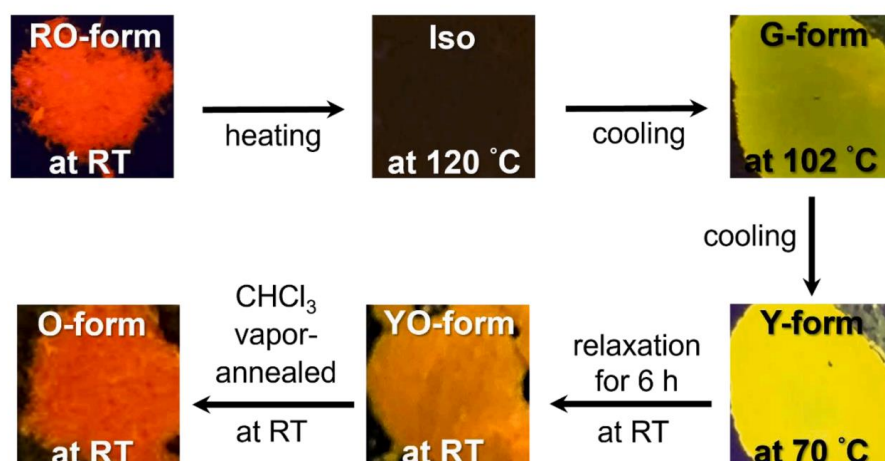


Fig. 1. Images illustrating the photoluminescence changes of **1** under excitation light at 365 nm at each temperature upon heating and cooling process.

Differential scanning calorimetry (DSC) analysis allowed us to verify the phase transition temperatures of **1**. Fig. 2 shows the traces of **1** at the first cooling and the second heating cycle run at 10 °C/min. Upon heating, **1** exhibited a single endothermic peak at 118.4 °C ($\Delta H = 26.9 \text{ kJmol}^{-1}$) corresponding to the isotropic point. Upon cooling, two exothermic peaks at 104.9 ($\Delta H = -20.4 \text{ kJmol}^{-1}$) and 98.4 °C ($\Delta H = -3.0 \text{ kJmol}^{-1}$) were witnessed which matched with the appearance temperatures of G-form and Y-form observed in Fig. 1, respectively. It indicates that the several crystalline forms of **1** could be obtained upon external stimuli and their type of organization influenced the photoluminescence colors, a feature which has never been observed from tetrazine derivatives reported so far.

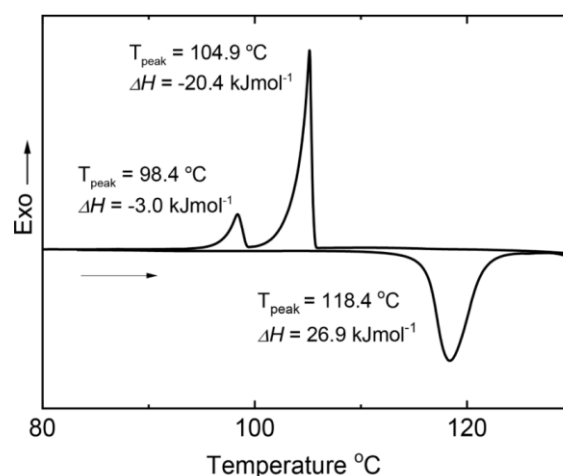


Fig. 2. DSC traces at the first cooling and the second heating cycle run at 10 °C/min.

The photophysical properties of **1** in solution and in the condensed states were investigated to obtain more insights into the thermoresponsive luminescence behavior. Table 1 and Fig S2 summarize the spectroscopic characteristics of **1** in solution states. Emission spectra and quantum yields were different depending on the organic solvents. In particular, when **1** was dissolved into an apolar solvent (*e.g.* cyclohexane), the compound was emissive because the intramolecular electron transfer is inhibited. However, in relatively polar solvents (*e.g.* DCM), the fluorescence was quenched, due to the existence of this electron transfer between the excited state localized on the tetrazine rings, and the donating side phenyl units. Dioxane which has a low polarity could be considered as an intermediate case, but despite THF has (in the Lippert-Mataga scale) almost the same polarity as DCM, **1** still exhibits fluorescence in this solvent. Thus, the solvent influence would clearly be more complex than a pure effect of polarity. Similar effects have been reported with completely different compounds [15].

	cyclohexane	dioxane	THF	DCM
λ_{abs} (nm)	541, 341	526, 344	529, 344	534, 339
λ_{em} (nm)	569	572	573	579
Stokes shift (cm^{-1})	880	1530	1450	1450
QY	0.29	0.11	0.095	0.01
Lifetime (ns)	150	57	46	n.d.

Table 1. Summary of photophysical properties of **1** in solution state.

When **1** was molecularly dispersed (no crystallites observed) in rigid polymer networks, such as polystyrene (PS) and poly(methyl methacrylate) (PMMA), it was emissive with fluorescence maxima at 583 and 570 nm, respectively (Fig. S3). **1**-doped polymer films show similar fluorescence decays that can be fitted with two long decay times: 91.2 and 38.1 ns for the PMMA film and 99 and 40 ns for the PS film (Table S2). Restricted intramolecular rotation upon dispersion in solid polymer matrices does not lead to significantly longer fluorescence decay times compared to the solution, contrary to what is commonly observed with AIE (Aggregation-induced emission) fluorophores.

Fig. 3 shows the absorption and photoluminescence spectra of **1** in different condensed states recorded at r.t. The emission spectrum of RO form (i) from the pristine crystals exhibited the reddish-orange emission with a band maximum at 600 nm. Thermal treatment at 120 °C resulted in the isotropization of **1** accompanying the luminescence quasiextinction. The most blue-shifted emission band appeared at 560 nm with shoulders at around 540 and 580 nm accompanying G-form (ii) which was isolated by supercooling to 5 °C from the melt state at 120 °C. Meanwhile, slow cooling of the melt to r.t. led to the Y-form (iii) with a single emission band at 567 nm. Subsequent slow relaxation of the sample at r.t. for 6 h resulted in the red-shift of the emission band (λ_{em} , max = 580 nm) with the appearance of a yellowish-orange emission color (YO-form, (iv)), with shoulders observed around 564 and 597 nm. Thermal annealing at 70 °C could facilitate this color shift. The Y-form and YO-form were however found metastable. Further red-shift of the emission band (λ_{em} , max = 592 nm) with shoulders around 574 nm and 610 nm could be obtained by chloroform vapor annealing at r.t. exhibiting deep orange photoluminescence appearance (O-form, (v)). Meanwhile, the photoluminescence spectrum of a single crystal of **1** (isolated from DCM) (Fig. S4) showed a single emission band at 610 nm which is the most red-shifted photoluminescence, while physical grinding of a single crystal with a spatula tip triggered a slight blue-shift of the band to 593 nm (Fig. S4). The emission lifetime analysis results shown in Table S3 provided us clues for this interesting spectral shift of **1** in the condensed state upon various thermal stimuli. The decay profiles could be fitted with double or triexponential decay functions. The lifetimes from broad spectra with shoulders were measured at various emission wavelengths. In the

G-form, short decay time species (2 ~ 3 ns and 12 ~ 14 ns) and longer decay time species of 22 ~ 24 ns were observed, with the ratio of the short ones increased clearly at 530 ~ 540 nm, an emission shoulder that can be associated with the green emitter, compared to other forms. From the red-shifted forms such as Y-form and YO-form, longer species over 20 ns appeared with a higher ratio and this was distinctive for longer emission wavelengths at 560 ~ 580 nm. Pristine RO-form exhibited a long emission lifetime of 22 ns at 600 nm with an almost pure red emitter. The emission decay time species of the isolated single crystal of **1** were 14.5 and 20.6 ns, and mechanical grinding of the single crystal triggered a slight decrease in the lifetimes to 13 and 19 ns (Table S3). This can be due to the increase in nonradiative deactivation due to the presence of more defects. Judging from the variations of lifetimes in each form, there would be three stable forms, displaying three distinct emission colors: green, red, and traditional orange emitters. In particular, we suggest that the longer lifetime species around 20 ns and 30 ns would correspond to the emission of mild excimer-like species that give orange and red photoluminescence, as proposed previously by previous workers, though with slightly different tetrazines [16,17] or possibly to dimeric structures existing in the ground state. In the G-form intermolecular interactions that stabilize more the ground state than the S1 state could tentatively explain the observed hypsochromic shift in fluorescence emission [18], although further structural analysis would be needed to fully confirm this hypothesis. However, this has never been observed before for tetrazine derivatives to the best of our knowledge, which opens a new track for the modulation of the photophysical properties in this exceptional family.

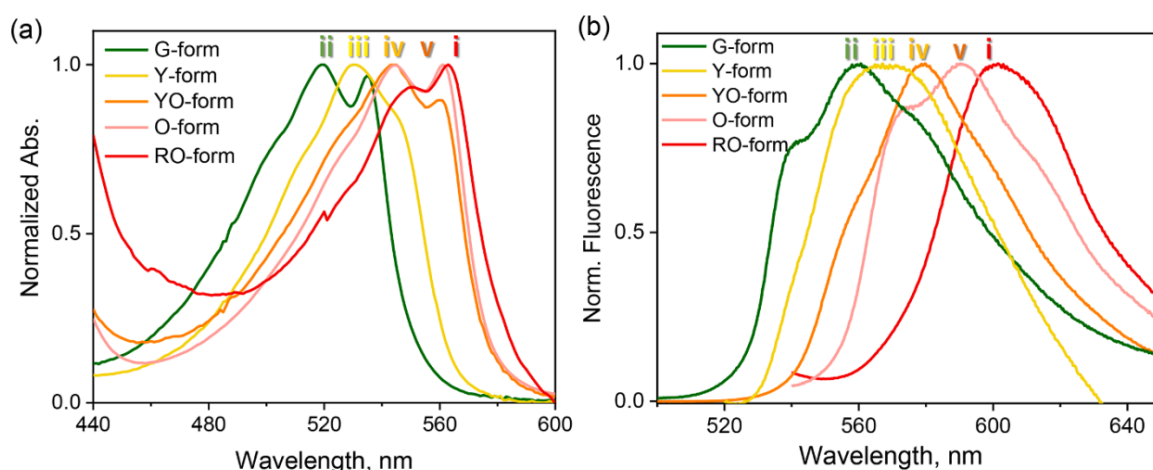


Fig. 3. (a) Absorption and (b) photoluminescence spectra of **1** in the condensed crystalline states measured at r.t.: i) Pristine RO-form, ii) G-form, iii) Y-form, iv) YO-form, and v) O-form (CHCl_3 vapor-annealed).

X-ray diffraction (XRD) measurements at r.t. were performed as shown in Fig. 4 to clarify the changes in the molecular assembled structure triggered by thermal treatment. The XRD diffractogram of pristine RO-form (e) has many sharp peaks reflecting its crystalline nature which was quite similar to that calculated from the single crystal analysis data (f). Indeed, it is highly probable that these two be the same crystalline phase, the absence of peaks in the 20-30° region in the RO form being linked to a favoured orientation of the crystal in the RO form powder, cancelling the appearance of the peaks in this region. Similarly, phase O (a) is probably also the same, since all displayed peaks have identical locations. The variations in the peak intensities between the O-form and the single crystal is likely due to the changing relative proportion of the crystalline defects.

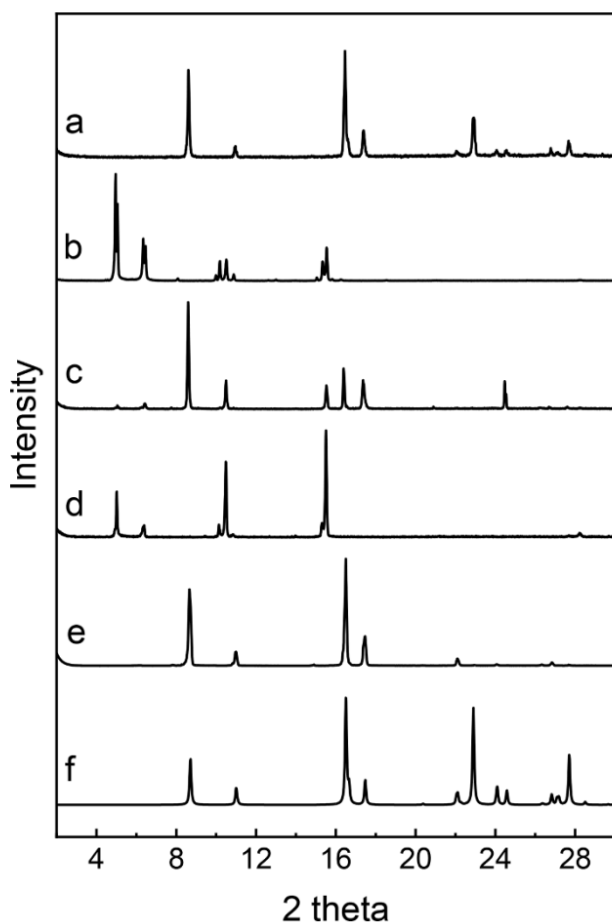


Fig. 4. X-ray diffraction patterns of the (a) O-form, (b) G-form, (c) YO-form, (d) Y-form, (e) RO-form, and (f) single crystal of **1**. All measurements were carried out at room temperature.

The first thermal treatment of RO-form resulted in very different diffraction patterns as observed from those of G-form (b) and Y-form (d), obtained after subsequent supercooling or slow cooling to r.t., respectively. This indicates the thermally-induced drastic change in the crystalline packing structures of **1**. The subsequent thermal annealing at 70°C afforded conversion to the YO-form (c). In the XRD pattern of YO form, several additional diffraction peaks which correspond to peaks present in pristine RO-form are observed. Thus, thermal annealing of the Y-form led to a much more stable crystalline structure, exhibiting an intermediate behavior with a yellowish- orange emission color comparable to mixed crystalline phases of pristine RO-form and Y-form. Further crystalline phase transition could be observed towards the O-form (a) by solvent-annealing of the YO-form with CHCl_3 vapor. The diffraction pattern was quite similar to the pristine state (or single crystal state) implying that the polymorphism of **1** is also responsive to the solvent exposure, which could almost restore the original packing structure and which is also consistent with the luminescence spectral shift close to RO-form. Meanwhile, taking a closer look at the Y- and YO-forms, it is interesting to observe that there is indeed one new “yellow phase” appearing, but which seems not to be pure. In the Y-form, this new “yellow phase” appears mixed with a certain amount of G-phase, on the other hand, the YO-form contains the new “yellow phase” along with some content of the O-phase. Therefore, surprisingly, while the G-form and both orange forms (O and RO) seem to be pure new phases, the Y and YO-forms are mixtures of the new yellow phase and other phases. Indeed, this latter yellow phase needs to be stabilized with small amounts of additional phases (G or O) but cannot be isolated pure. Moreover, it is even possible, from the existence of a new unique peak at 24°, that it is not one, but two new yellow forms that are

coexisting (along with the G and O together), although an explanation involving crystalline defects cannot be ruled out.

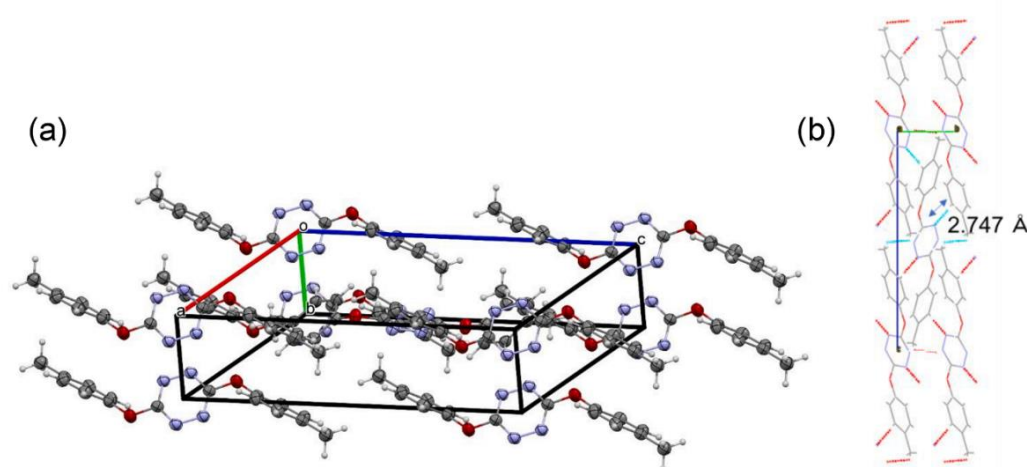


Fig. 5. (a) Crystal structure of **1**. (b) Overlap of **1** molecules viewed from normal to the molecular plane.

X-ray single crystallography analysis of **1** (Fig. 5) reveals that there exists π - π interaction (spacing of 4.162 Å) and C-H \cdots π interaction (the shortest distance of 2.747 Å) involving methyl group in the molecular packing structure of **1**. This kind of T-shape (perpendicular arrangement) interaction is known to exhibit the most stable and the lowest energy packing by forming mild excimers [16,17]. This is also consistent with the fact that the photoluminescence of the single crystal showed the most red-shifted red emission at 610 nm (Fig. S4). Meanwhile, we could observe another surprising feature - the existence of mechanical flexibility in a large crystal- of **1**. Common small molecules-based crystals are easily fractured by physical forces like pressing or bending, due to their brittleness. However, **1** exhibited quite important bendability, as shown in Fig. 6 (See ESI for the video clip). The examined crystal size was a length of 5.13 cm, a width of 200 μm , and a thickness of 50 μm . When one end was fixed with a scotch tape on the substrate and the other end was forced with a spatula tip, it showed bending motions in three directions. The largest bending angle was 37° (Fig. 6b) and the bending radius of 985 μm (Fig. 6c). Combination of weak interactions and CH- interactions results in isotropic interactions in the crystal packing, a feature that has been shown to be favorable for crystal elasticity since it allows molecular movement within the crystal lattice [19,20].



Fig. 6. Mechanically flexible characteristics of long crystal of **1**. Crystal size: 5.13 cm (length) \times 200 μm (width) \times 50 μm (thickness).

4. Conclusions

In conclusion, we demonstrate that bis(4-methylphenoxy)tetrazine (**1**) exhibits external stimuli-responsive emission colors in the condensed state. Several crystalline forms of **1** could be obtained

upon thermal treatment and their type of organization influenced the photoluminescence colors of green, yellow and red in addition to the traditional orange color. Polymorphism of **1** was also responsive to solvent vapor exposure, which could almost restore the original packing structure as well as its photoluminescence spectrum. In addition, mechanical flexibility in a large crystal of **1** was observed which possibly originated from the weak interactions and CH \cdots interactions in the crystal packing. To the best of our knowledge, this is the first example of s-tetrazine derivatives exhibiting external stimulus-tunable multi-photoluminescence colors and flexibility in crystalline states which would open a new chapter of the exceptional s-tetrazine family.

CRediT authorship contribution statement

Yuna Kim: Conceptualization, Data curation, Investigation, Project administration, Resources, Software, Supervision, Validation, Writing – original draft, Writing – review & editing. **Clémence Allain:** Conceptualization, Data curation, Investigation, Project administration, Resources, Software, Supervision, Validation, Writing – original draft, Writing – review & editing. **Régis Guillot:** Data curation, Investigation, Resources, Software, Writing – original draft. **Pierre Audebert:** Conceptualization, Investigation, Validation, Writing – original draft, Writing – review & editing.

Declaration of Competing Interest The authors declare that they have no known competing financial interests or personal relationships that could have appeared to influence the work reported in this paper.

Data availability : Data will be made available on request.

Acknowledgment : The support of the president grant for promoting overseas research and education exchange from Hokkaido University and the 3C Fund from Utsunomiya University are appreciated, as well as an invited professorship position in ENS Paris-Saclay for YK.

Supplementary data The crystal data collection and refinement parameters are described. Excitation and emission spectra of **1** in a molecularly dispersed and rigidified state in the PMMA or PS network are featured with a table of summarized photophysical properties. Emission spectra of a single crystal of **1** and its ground state, and the summarized table of emission lifetimes of **1** in different forms are available. A video showing the bendability of a large crystal is also available online. Supplementary data to this article can be found online at

<https://doi.org/10.1016/j.jphotochem.2023.114629>.

References

- [1] G. Clavier, P. Audebert, s-Tetrazines as Building Blocks for New Functional Molecules and Molecular Materials, *Chem. Rev.* 110 (6) (2010) 3299–3314.
- [2] P. Audebert, F. Miomandre, 1,2,4,5-Tetrazines: An intriguing heterocycles family with outstanding characteristics in the field of luminescence and electrochemistry, *J. Photochem. Photobiol. Photochem. Reviews* 44 (2020), 100372.
- [3] Y. Kim, E. Kim, G. Clavier, P. Audebert, New tetrazine-based fluoro-electrochromic window; modulation of the fluorescence through applied potential, *Chem. Commun.* 34 (2006) 3612–3614.
- [4] Y. Kim, J. Do, E. Kim, G. Clavier, L. Galmiche, P. Audebert, Tetrazine-based electrofluorochromic windows: modulation of the fluorescence through applied potential, *J. Electroanal. Chem.* 632 (2009) 201–205.
- [5] S. Seo, Y. Kim, Q. Zhou, G. Clavier, P. Audebert, E. Kim, White electrofluorescence switching from electrochemically convertible yellow fluorescent dyad, *Adv. Funct. Mater.* 22 (17) (2012) 3556–3561.
- [6] J.P. Calupitan, A. Brosseau, P. Josse, C. Cabanetos, J. Roncali, R. Métivier, C. Allain, Mechanofluorochromic Material toward a Recoverable Microscale Force Sensor, *Adv. Mater. Interfaces* 9 (2022) 2102246.
- [7] Y. Sagara, M. Karman, E. Verde-Sesto, K. Matsuo, Y. Kim, N. Tamaoki, C. Weder, Rotaxanes as mechanochromic fluorescent force transducers in polymers, *J. Am. Chem. Soc.* 140 (5) (2018) 1584–1587.
- [8] G. Zhang, J. Lu, M. Sabat, C.L. Fraser, Polymorphism and Reversible Mechanochromic Luminescence for

- Solid-State Difluoroboron Avobenzene, *J. Am. Chem. Soc.* 132 (7) (2010) 2160–2162.
- [9] E. Jullien-Macchi, V. Alain-Rizzo, C. Allain, C. Dumas-Verdes, P. Audebert, sTetrazines functionalized with phenols: synthesis and physico-chemical properties, *RSC Adv.* 4 (2014) 34127–34133.
- [10] Q. Zhou, P. Audebert, G. Clavier, R. Meallet-Renault, F. Miomandre, Z. Shaukat, T.-T. Vu, J. Tang, New Tetrazines Functionalized with Electrochemically and Optically Active Groups: Electrochemical and Photoluminescence Properties, *J. Phys. Chem. C* 115 (44) (2011) 21899–21906.
- [11] G.M. Sheldrick, SHELXS-97, University of Gottingen, Gottingen, Germany, Program for Crystal Structure Solution, 1997.
- [12] G.M. Sheldrick, A short history of SHELX, *Acta Crystallogr. Sect. A: Found. Crystallogr.* 64 (1) (2008) 112–122.
- [13] L.J. Farrugia, WinGX suite for small-molecule single-crystal crystallography, *J. Appl. Cryst.* 32 (4) (1999) 837–838.
- [14] F. Miomandre, G. Clavier, M.C. Vernieres, S. Badré, R. Meallet-Renault, Synthesis and Properties of New Tetrazines Substituted by Heteroatoms: Towards the World's Smallest Organic Fluorophores, *Chem. Eur. J.* 11 (2005) 5667–5673.
- [15] P.K. Ghorai, D.V. Matyushov, Solvent Reorganization Entropy of Electron Transfer in Polar Solvents, *J. Phys. Chem A* 110 (2006) 12363–12371.
- [16] D.V. Brumbaugh, C.A. Haynam, D.H. Levy, Mild excimers: The spectrum of the dimethyl-tetrazine dimer, *J. Chem. Phys.* 73 (1980) 5380–5381.
- [17] J. Pawliszyn, M.M. Szczesniak, S. Schemer, Interactions between Aromatic Systems: Dimers of Benzene and s-Tetrazine, *J. Phys. Chem.* 88 (1984) 1726–1730.
- [18] C.L. Morter, A. Koskelo, Y.R. Wu, D.H. Levy, The electronic spectra and structure of complexes between s-tetrazine and acetylene, *J. Chem. Phys.* 89 (4) (1988) 1867–1875.
- [19] A.J. Thompson, A.I. Chamorro Oru'e, A.J. Nair, J.R. Price, J. McMurtrie, J.K. Clegg, Elastically flexible molecular crystals, *Chem. Soc. Rev.* 50 (21) (2021) 11725–11740.
- [20] S. Ghosh, M.K. Mishra, Elastic Molecular Crystals: From Serendipity to Design to Applications, *Cryst. Growth Des.* 21 (4) (2021) 2566–2580.